Pergamon

0956-7151(94)00302-5

Acta metall. mater. Vol. 43, No. 3, pp. 1023–1028, 1995

0956-7151/95 $9.50 + 0.00

TEXTURE SIMULATION FOR HOT ROLLING OF ALUMINIUM BY USE OF A TAYLOR MODEL CONSIDERING GRAIN INTERACTIONS

D. RAABE

Institut für Metallkunde und Metallphysik, RWTH Aachen, Kopernikusstrasse 14, 52056 Aachen, Germany

(Received 18 November 1993; in revised form 20 June 1994)

Abstract—The hot rolling textures of aluminium are simulated by means of a Taylor type model which takes into consideration dislocation slip on {111}⟨110⟩ and {110}⟨110⟩ glide systems and the interaction of grains. For the investigation of the stability of the cube component during hot rolling various ratios of the corresponding critical resolved shear stresses $\tau^{\{110\}}/\tau^{\{111\}}$ are applied. Whereas the orientation densities and the positions of the β-fibre components {112}⟨111⟩ and {123}⟨634⟩ are not substantially influenced by slip on {110}⟨110⟩ glide systems the cube component is developed at the expense of the {110}⟨112⟩ orientation when the yield surface for {110} slip is within that for {111} slip.

Résumé—Les textures de laminage à chaud de l'aluminium ont été simulées à l'aide d'un modèle de Taylor tenant compte des systèmes de glissements {111}⟨110⟩ et {110}⟨110⟩ aussi que des interactions entre grains adjacents. Pour étudier la stabilité d'orientation cube pendant le laminage à chaud, on a appliqué différents rapports de contrainte de cisaillement $\tau^{\{110\}}/\tau^{\{111\}}$. Tandis que les densités d'orientation et les positions des composantes {112}⟨111⟩ et {123}⟨634⟩ de la β-fibre ne sont que faiblement affectées par le glissement sur le système {110}⟨110⟩, la composante cube se développe aux dépens de l'orientation {110}⟨112⟩ lorsque limite élastique pour le glissement {110} se trouve dans le limite éastique du glissement {111}.

Zusammenfassung—Die Warmwalztexturen von Aluminium sind mit Hilfe eines Taylormodelles, welches sowohl {111}⟨110⟩ und {110}⟨110⟩ Gleitsysteme, als auch die Wechselwirkung zwischen Körnern berücksichtigt, simuliert worden. Zur Untersuchung der Stabilität der Würfellage während des Warmwalzens wurden verschiedene Verhältnisse der kritischen Schubspannungen $\tau^{\{110\}}/\tau^{\{111\}}$ verwendet. Während die Orientierungsdichten und die Positionen der β-Faserkomponenten {112}⟨111⟩ und {123}⟨634⟩ nur wenig von der Aktivierung der {110}⟨110⟩ Gleitsysteme betroffen werden, entwickelt sich die Würfellage auf Kosten der {110}⟨112⟩ Komponente, wenn die Fließfläche für {110} Gleitung innerhalb der für {111} Gleitung liegt.

1. INTRODUCTION

The cube component {001}⟨100⟩ is the dominant recrystallization component of the crystallographic texture in strongly cold rolled and subsequently annealed face centered cubic (f.c.c.) materials with high and medium stacking fault energy. The origin of grains with this orientation has been the subject of thorough investigations in the past, e.g. [1, 2]. By examination of the local texture by means of transmission electron microscopy [3] and analysis of electron back scattering patterns in the scanning electron microscope [2] it was revealed that elongated cube-oriented zones occur in the microstructure of cold rolled copper [3] and aluminium [2, 4]. These cube-oriented ribbon-like zones, which have been interpreted as transition bands [5] are supposed to act as nuclei during subsequent recrystallization.

Whereas special attention has thus been drawn to the explanation of the formation of cube oriented zones in cold rolled aluminium, the evolution of cube-oriented grains during hot rolling has often been neglected. According to slip traces which were found in hot rolled aluminium [6–8] the activation of dislocation slip not only on {111}⟨110⟩ slip systems but additionally on {110}⟨110⟩ systems must be taken into account for homologous rolling temperatures above 0.6. Recently the stability of cube-oriented grains during hot rolling of aluminium has therefore been inspected by use of Taylor simulations considering slip on all potential slip systems [8, 9] and by experimental investigation of hot rolled aluminium single crystals with initial {001}⟨100⟩ and {001}⟨110⟩ orientations [8].

While in the Taylor simulations by Bacroix and Jonas [9] the cube component did not occur at all, in the work of Maurice and Driver [8], who assumed a pancake-like grain morphology and therefore applied the corresponding "Relaxed Constraints" Taylor

type model (RC) [10], the predicted cube orientation was very strong.

In the present work the attempt was thus made to submit a more realistic Taylor simulation for hot rolling of aluminium which on the one hand takes into account $\{111\}\langle 110\rangle$ and $\{110\}\langle 110\rangle$ slip systems [6–8] and on the other hand considers the orientation dependent interaction between neighbouring grains as proposed by Schmitter *et al.* [11] instead of generally relaxing the corresponding shears as earlier suggested by the RC models [10].

2. SIMULATION METHOD

For the simulation of crystallographic rolling textures mainly two types of Taylor models have been in use in the past. In the "Full Constraints" Taylor models (FC) [12] the externally imposed strain tensor is entirely transferred into each grain where it has to be accomplished by crystallographic slip (or/and twinning). This concept assures the avoidance of incompatibilities between grains. In the RC Taylor type models which were proposed by Honneff and Mecking [10] some of the imposed shear components need not to be fulfilled, i.e. they are relaxed. This assumption allows for local incompatibilities between neighbouring grains and leads to the reduction of the number of employed slip systems and hence to a lower deformation energy (Taylor energy) as compared to the FC model. The RC models are of relevance for high degrees of deformation, since then the so called lath or respectively pancake like shapes of the grains cause only little mutual interaction.

In the new Taylor type approach by Schmitter *et al.* [11], however, the shears are only partially relaxed according to the gain in deformation energy which depends on the orientations of the grain. This shear dependent decrease of the Taylor energy is expressed by the so called shear capacity, which is defined as the maximum slope of the plane which combines the deformation energy predicted by the FC model with that computed by the RC model [11]. The shear capacity is thus dependent on the orientation of the grain and is a measure for the gain in energy that is achieved if a certain shear component is relaxed. Whereas this approach can even analytically be solved for arbitrary combinations of two grains in the two-dimensional case [11] an exact consideration of the interaction between neighbouring grains in the three-dimensional case leads to very long computation times. A simplified approach for the orientation dependent, partial relaxation of shears was thus made by Wagner *et al.* [11, 13] for the three-dimensional case. In this approximation the shear capacities are calculated independently for the three possible shear components. These values are normalized by the highest occurring shear capacity for the corresponding shear. This approach leads to a better description of the rolling textures of f.c.c. metals as compared to the predictions of the current FC or RC models [11].

In order to tackle hot rolling of aluminium in the present work $\{111\}\langle 110\rangle$ and $\{110\}\langle 110\rangle$ slip systems are taken into consideration. The ratio between the critical resolved shear stress (CRSS) on $\{110\}$ and $\{111\}$ slip planes, $\alpha = \tau^{\{110\}}/\tau^{\{111\}}$, is varied according to the results of Maurice and Driver [8]. In their work the calculation of the yield surfaces of the cube component according to both types of slip systems suggested that, if $\alpha < \sqrt{(3/2)}$, slip on $\{110\}$ is the dominant deformation mechanism. From their experiments Maurice and Driver [8] found that a transition of the selected type of slip systems occurs at 300°C. While at 400°C only $\{110\}\langle 110\rangle$ slip was observed, at 200°C exclusively $\{111\}\langle 110\rangle$ slip traces were found. At 300°C, however, slip lines stemming from both types of slip systems were detected.

In the present, work simulations are carried out for CRSS ratios $\alpha = 0.3, 0.77, 1.0, 1.3$ and 3.0. According to the simulation of hot rolling an external ideal plane strain state is imposed. The rolling textures are computed in $\Delta\varepsilon_{11} = 0.01$ steps up to a total deformation of $\varepsilon_{11} = 2.3$, starting from an initially random texture consisting of 936 single orientations. As second order plastic criterion the approach of Renouard and Winterberger is used [14].

3. RESULTS AND EVALUATION

The simulated textures are presented by means of φ_2-sections through the reduced Euler space ($0° \leqslant \phi_1, \phi, \varphi_2 \leqslant 90°$C) in $\Delta\varphi_2 = 5°$ steps. Relevant orientations of f.c.c. rolling textures are shown in Fig. 1. For the texture description mainly three fibres are important, namely the α-fibre, which comprises all orientations between $\{011\}\langle 100\rangle$ (Goss) and

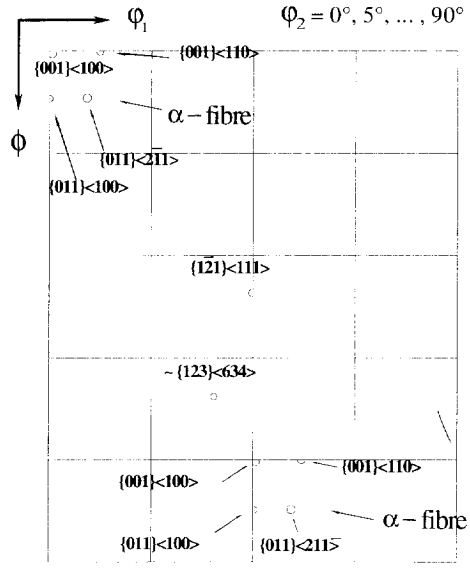

Fig. 1. Some relevant texture components and fibres for hot rolling of aluminium, schematical presentation in φ_2 sections.

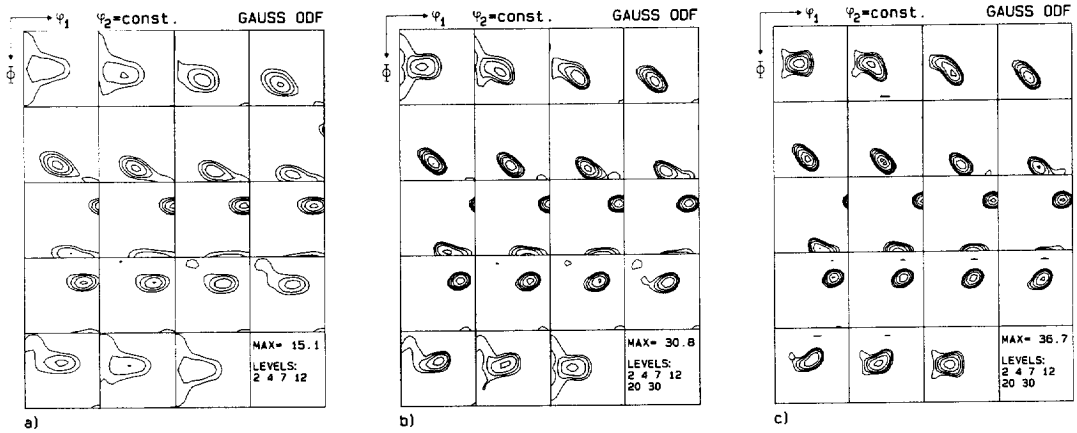

Fig. 2. Simulated rolling textures for low temperature deformation of aluminium according to the Schmitter model [11], consideration of {111}⟨110⟩ slip systems. (a) $\varepsilon_{11} = 0.51$, (b) $\varepsilon_{11} = 1.20$, (c) $\varepsilon_{11} = 2.30$.

{111}⟨110⟩, including {011}⟨211⟩ (*B* orientation), the β-fibre which includes {112}⟨111⟩ (*C* component), {123}⟨634⟩ (*S* component) and the *B* component and the cube-fibre which is located between the Cube and the Goss orientation.

In Fig. 2 the simulated rolling textures are shown for low temperature deformation of aluminium, i.e. only the 12 {111}⟨110⟩ slip systems are taken into account. After $\varepsilon_{11} = 0.51$ a weak α-fibre and a stronger β-fibre are developed, Fig. 2(a). Additionally a weak cube-fibre appears. After $\varepsilon_{11} = 1.2$, Fig. 2(b), the cube component is rotated about the rolling direction and the β-fibre, especially the *C* and the *S* component are stronger. With increasing rolling deformation, Fig. 2(c), $\varepsilon_{11} = 2.3$, the β-fibre, especially the *B* orientation, which is not sufficiently pronounced in RC-pancake simulations, is increased. As pointed out by Schmitter [11], Wagner [13] and Hirsch [15] this texture evolution corresponds to the experimentally found rolling textures of pure aluminium more precisely than the predictions yielded by the FC or RC models. Reasonable results are thus also anticipated for texture predictions on the basis of additionally considered {110}⟨110⟩ slip systems.

In Fig. 3 the simulation which accounts for slip on {111}⟨110⟩ and {110}⟨110⟩ glide systems (identical CRSS on both systems, $\alpha = 1$, $\tau^{\{110\}} = \tau^{\{111\}}$) and thus corresponds to high temperature deformation of aluminium [6–8], is presented. Although basically the same type of texture including the *C*-, *S*- and *B*-components is developed as compared to the low temperature simulation including only {111}⟨110⟩ slip systems, Fig. 2, additionally a pronounced cube component is generated, Table 1. It is thus shown by this simulation that not only the stability of pre-existing cube oriented grains is confirmed by slip on {110}⟨110⟩ systems as stated by Maurice and Driver [8] but that additionally the evolution of new cube grains can be explained. In comparison to the simulation with slip on {111}⟨110⟩ glide systems, Fig. 2, the here predicted orientation density of the *B* component is nearly unchanged, Fig. 3(c), Table 1. That means there is nearly no decrease of the *B* orientation at the expense of the competitively developing cube component. It has, however, to be recognized that especially after $\varepsilon_{11} = 1.2$, Fig. 3(b), and $\varepsilon_{11} = 2.3$, Fig. 3(c), the cube component is ≈ 10–$15°$ rotated about the rolling direction, Table 1. As also

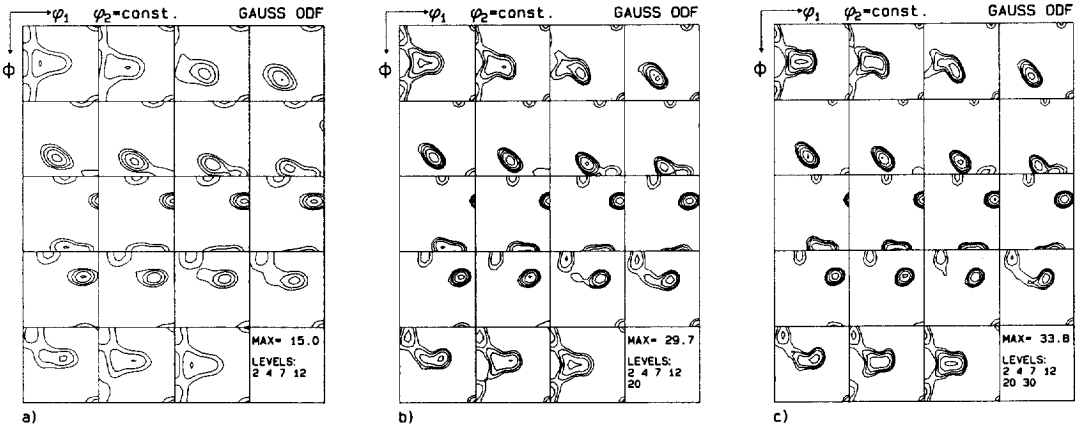

Fig. 3. Simulated rolling textures for high temperature deformation of aluminium according to the Schmitter model [11], consideration of {111}⟨110⟩ and {110}⟨110⟩ slip systems, $\tau^{(110)}/\tau^{(111)} = 1.0$. (a) $\varepsilon_{11} = 0.51$, (b) $\varepsilon_{11} = 1.20$, (c) $\varepsilon_{11} = 2.30$.

Table 1. Predicted orientation densities for relevant components according to various simulations accounting for grain interaction

	f.c.c., conventional			Aluminium, hot rolling, $\alpha = 0.33$			Aluminium, hot rolling, $\alpha = 0.77$			Aluminium, hot rolling, $\alpha = 1.0$			Aluminium, hot rolling, $\alpha = 1.3$		
ε_{11}	0.51	1.20	2.30	0.51	1.20	2.30	0.51	1.20	2.30	0.51	1.20	2.30	0.51	1.20	2.30
Cube	1.9	1.1	0.8	3.9	3.9	3.3	5.1	6.0	5.7	5.1	6.3	5.5	2.7	2.0	0.8
Cube (rot.)	3.0	3.2	1.5	5.3	8.6	7.1	6.1	8.8	8.4	6.0	9.3	8.6	3.3	3.9	1.9
B	6.7	14.3	27.4	8.3	10.0	10.8	6.4	9.6	16.8	6.9	13.8	22.3	7.1	14.8	30.4
C	14.8	30.8	36.7	15.7	34.4	46.4	15.1	30.5	34.9	15.0	29.7	33.8	15.0	30.7	35.3
S	12.6	25.5	28.6	11.5	22.3	29.0	11.8	22.4	15.5	11.5	20.6	21.3	11.7	21.3	22.0

ε_{11} = simulated rolling deformation, true strain.
Cube = f (g) of the "Cube" component, $\{001\}\langle 100\rangle$.
Cube (rot.) = f (g) of the "Cube" component, rotated 10–15° about the rolling direction, $\approx\{015\}\langle 100\rangle$.
$B = f$ (g) of the "Brass" component, $\approx\{011\}\langle 211\rangle$ (φ_1 within the range 25–35°).
$C = f$ (g) of the "Copper" component, $\approx\{112\}\langle 111\rangle$.
$S = f$ (g) of the "S" component, $\approx\{123\}\langle 634\rangle$.
Conventional = consideration of $\{111\}\langle 110\rangle$ slip systems only.
Hot rolling = consideration of $\{111\}\langle 110\rangle$ and $\{110\}\langle 110\rangle$ slip systems.
α = ratio between critical resolved shear stress on $\{110\}\langle 110\rangle$ and $\{111\}\langle 110\rangle$ slip systems, $\alpha = \tau^{\{110\}}/\tau^{\{111\}}$.

found by Maurice and Driver [8] the formation of the $\{001\}\langle 110\rangle$ component is not affected by slip on $\{110\}\langle 110\rangle$.

For $\alpha > \sqrt{(3/2)}$ Maurice and Driver [8] showed, that the yield surface for $\{110\}$ slip is outside that for $\{111\}$ slip, i.e. $\{110\}$ systems are not critically stressed. In this case slip only occurs on $\{111\}$ planes. In the following simulation this result was examined by assuming a slightly higher value of $\alpha = 1.3$, Fig. 4. It comes out that the texture evolution in this case is even in details very similar to that, which is predicted by activation of only 12 $\{111\}\langle 110\rangle$ slip systems, Fig. 2, Table 1. Even the maximum orientation density of both calculations is nearly identical. It is hence concluded, that for $\alpha > \sqrt{(3/2)}$ slip on $\{110\}\langle 110\rangle$ systems does not contribute to deformation. This is also confirmed by simulations carried out with $\alpha = 3$ which exactly yield the same results as those with $\alpha = 1.3$.

For $\alpha = 0.77$, i.e. $\tau^{\{111\}} = 1.3 \times \tau^{\{110\}}$, the yield surface for slip on $\{110\}$ glide planes is completely inside that for $\{111\}$ slip, i.e. the $\{110\}$ systems are critically stressed. This is established by the corresponding simulations, Fig. 5. It is shown that the cube orientation is again formed at the expense of the *B* component, Table 1. The general shape of the ODF, the orientation density of the cube orientation and the maximum intensity of the *C* component are very similar to the predictions of the simulations with $\alpha = 1.0$, Fig. 3.

For $\alpha = 0.33$, Fig. 6, the cube orientation is weaker than in the simulations with $\alpha = 0.77$, Fig. 5, Table 1. Whereas for $\alpha = 0.77$, Fig. 5, and $\alpha = 1.0$, Fig. 3, the maximum of the cube component deviates at most 10° from its exact position ($\varphi_1 = 0°$, $\phi = 0°$, $\varphi_2 = 0°$) in the present simulation ($\alpha = 0.33$) it is rotated and spread about the rolling direction towards the Goss component, Fig. 6. This cube-fibre is formed at the expense of the *B* orientation, whereas the orientation density of the *C* component is considerably increased, Table 1.

The course of the simulated orientation density of the exact cube component, $\{001\}\langle 100\rangle$, and of the rotated cube component, $\approx\{015\}\langle 100\rangle$, is depicted in Fig. 7 as function of α for various strains. The maximum intensity of both components is developed for α values within the range 0.77–1.0 for all inspected rolling degrees. If α is lower than 0.77 or higher than 1.0 the cube component decreases. It is additionally shown that the rotated cube orientation,

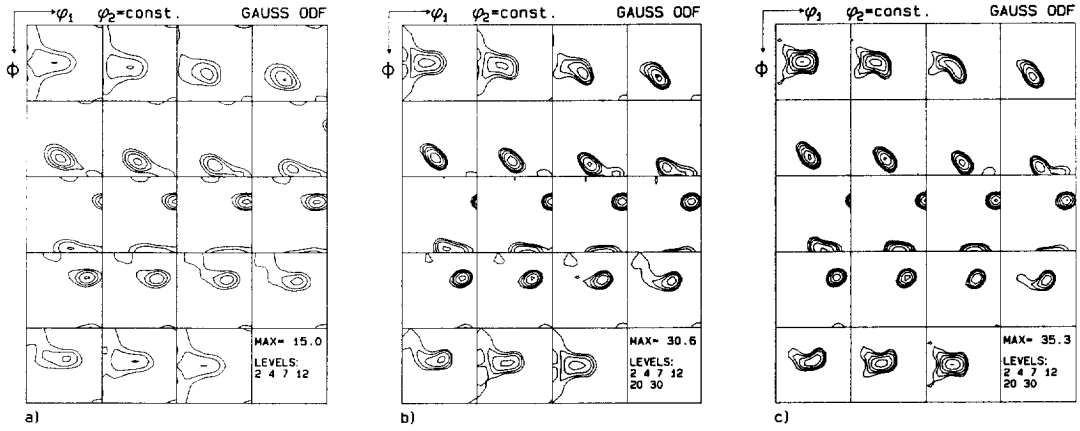

Fig. 4. Simulated rolling textures for high temperature deformation of aluminium according to the Schmitter model [11], consideration of $\{111\}\langle 110\rangle$ and $\{110\}\langle 110\rangle$ slip systems, $\tau^{\{110\}}/\tau^{\{111\}} = 1.3$. (a) $\varepsilon_{11} = 0.51$, (b) $\varepsilon_{11} = 1.20$, (c) $\varepsilon_{11} = 2.30$.

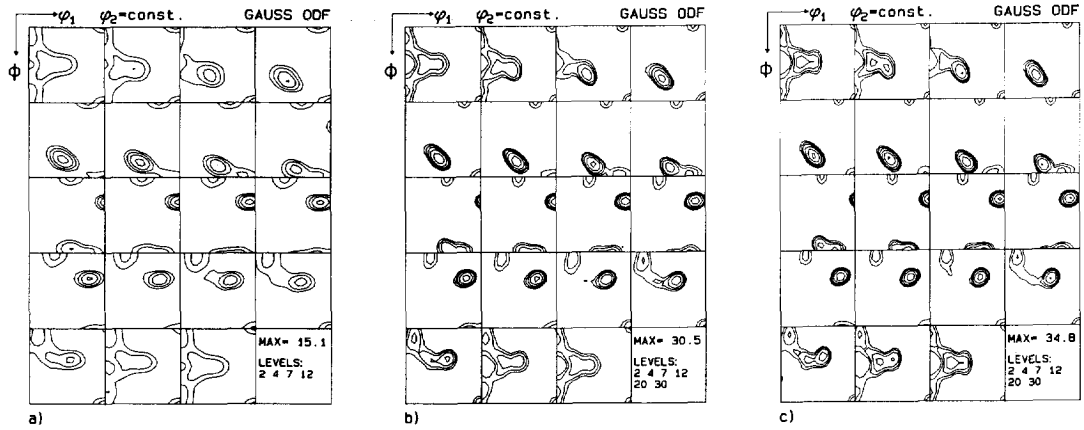

Fig. 5. Simulated rolling textures for high temperature deformation of aluminium according to the Schmitter model [11], consideration of {111}⟨110⟩ and {110}⟨110⟩ slip systems, $\tau^{(110)}/\tau^{(111)} = 0.77$. (a) $\varepsilon_{11} = 0.51$, (b) $\varepsilon_{11} = 1.20$, (c) $\varepsilon_{11} = 2.30$.

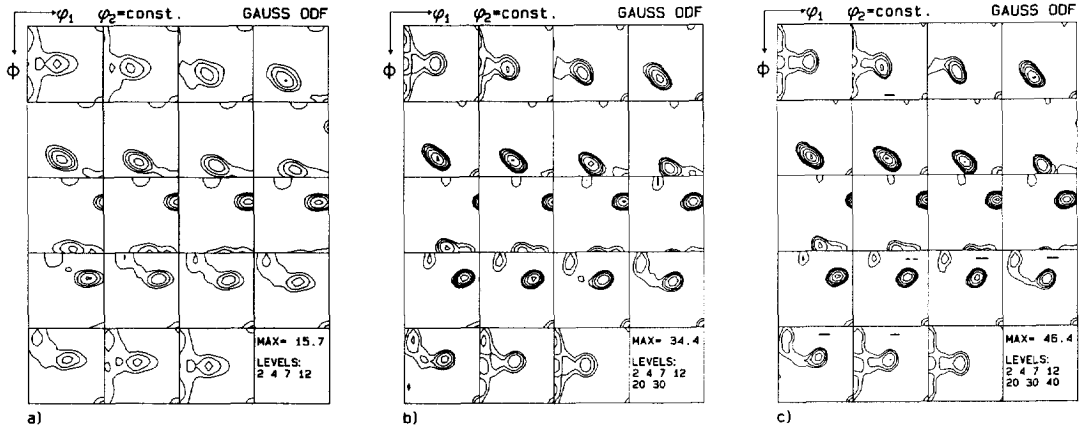

Fig. 6. Simulated rolling textures for high temperature deformation of aluminium according to the Schmitter model [11], consideration of {111}⟨110⟩ and {110}⟨110⟩ slip systems, $\tau^{(110)}/\tau^{(111)} = 0.33$. (a) $\varepsilon_{11} = 0.51$, (b) $\varepsilon_{11} = 1.20$, (c) $\varepsilon_{11} = 2.30$.

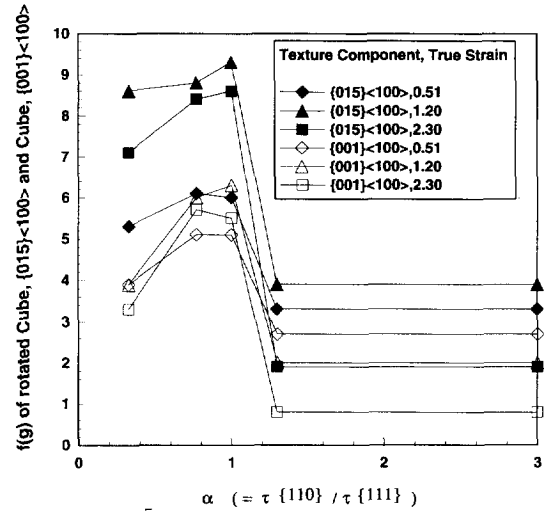

Fig. 7. Course of the simulated orientation density of the exact cube component, {001}⟨100⟩, and of the rotated cube component, ≈{015}⟨100⟩, as function of α for various strains.

≈{015}⟨110⟩, is generally stronger than the exact cube component.

4. CONCLUSIONS

The generation of the cube texture component during hot rolling of aluminium can be successfully simulated by means of a Taylor type model which takes into consideration dislocation slip on {111}⟨110⟩ and {110}⟨110⟩ glide systems on the one hand and—in a recently introduced simplified approach—the interaction of neighbouring grains on the other hand. The maximum of the cube component is revealed for $\tau^{\{110\}}/\tau^{\{111\}}$ ratios within the range 0.77–1.0. The maximum of this component is, however, permanently shifted ≈10–15° about the rolling direction. While the maximum orientation densities and the exact positions of the *C* and of the *S* component are only weakly influenced by {110}⟨110⟩ slip the *B* orientation is decreased with the increase of the cube fibre. The texture component

$\{001\}\langle 110\rangle$ is not affected by activation of slip on $\{110\}\langle 110\rangle$ systems.

REFERENCES

1. W. Köster, *Zeit. Metallkunde* **18,** 112 (1926).
2. J. Hjelen, R. Ørsund and E. Nes, *Acta. metall. mater.* **39,** 1377 (1991).
3. B. J. Duggan, M. Sindel, G. D. Köhlhoff and K. Lücke, *Acta metall. mater.* **38,** 103 (1990).
4. A. L. Dons and E. Nes, *Mater. Sci. Technol.* **2,** 8 (1986).
5. I. L. Dillamore and H. Katoh, *Metal Sci.* **8,** 71 (1974).
6. R. Le Hazif, P. Dorizzi and J. P. Poirier, *Acta metall.* **21,** 903 (1973).
7. R. Le Hazif and J. P. Poirier, *Acta metall.* **23,** 865 (1975).
8. Cl. Maurice and J. H. Driver, *Acta metall. mater.* **41,** 1653 (1993).
9. B. Bacroix and J. J. Jonas, *Text. Microstruct.* **8–9,** 267 (1988).
10. H. Honneff and H. Mecking, *Proc. 5th Int. Conf. Tex. Mater. ICOTOM 5* (edited by G. Gottstein and K. Lücke), p. 265, Springer, Berlin (1978) and *Proc. 6th Int. Conf. Tex. of Mat. ICOTOM 6* (edited by P. ISIJ), p. 347. Tokyo (1981).
11. U. Schmitter, P. Wagner and K. Lücke, *Proc. 4th Int. Symp. on Plasticity and its Current Applications.* Baltimore (1993).
12. G. I. Taylor, *J. Inst. Metals* **61,** 307 (1938).
13. P. Wagner, U. Schmitter and K. Lücke, *Mat. Sci. Forum* 157–162, part 2, p. 1777 (1994).
14. M. Renouard and M. Wintenberger, *C.r. Acad. Sci.* **B283,** 237 (1976).
15. J. Hirsch, *Proc. 10th Int. Conf. on Tex. of Mat. ICOTOM 10.* Clausthal (1993).